ORIGINAL PAPER

MICROSTRUCTURAL AND MECHANICAL CHARACTERIZATION OF 301 STAINLESS STEEL WELDED JOINTS

AURORA POINESCU[1], SIMONA MIHAI[2], IOAN ALIN BUCURICA[2], IOANA DANIELA DULAMA[2], SOFIA TEODORESCU[2]

Manuscript received: 17.11.2017; Accepted paper: 12.01.2018;
Published online: 30.03.2018.

Abstract. *Changes in structure, chemical composition and volume occurring in fusion welding have a decisive influence on the properties of welded joints. In this study, were performed microstructural and mechanical characterizations on weld 301 stainless steel.*
Keywords: *words welding zone, SEM-EDS, AFM, nanoindentation, stainless steel.*

1. INTRODUCTION

Austenitic steels are characterized by their high content of austenite-formers, especially nickel. They are also alloyed with chromium, molybdenum and sometimes with copper, titanium, niobium and nitrogen. Alloying with nitrogen raises the yield strength of the steels. The molybdenum-free steels also have very good high-temperature properties and are therefore used in furnaces and heat exchangers. Their good impact strength at low temperatures is often exploited in vessels for cryogenic liquids [1].

Stainless steel type 301 is part of austenitic stainless steels. This alloy is non-magnetic in annealed condition, but becomes magnetic when is cold worked. High mechanical strength and corrosion resistance are excellent properties of these materials and are required in many applications such as: aircraft structural parts, structural parts of machines, utensils, containers, equipment enclosures.

Welds in Grade 301 must be annealed for maximum corrosion resistance - this is not necessary in 301L or 301LN. Welding and post weld annealing will both remove high strength induced by prior cold rolling. Spot welding is commonly used to assemble cold rolled 301 components. The very small heat affected zone associated with this rapid welding technique results in little reduction of overall component strength [2]. Metallurgical weld quality depends on various factors as: structure, chemichal composition, design (e.g. geometry and shape of pieces), and technological (e.g. welding parameters).

Steel and weld metal with high chromium and molybdenum contents may undergo precipitation of brittle sigma phase in their microstructure if they are exposed to high temperatures for a certain length of time. The transformation from ferrite to sigma or directly from austenite to sigma proceeds most rapidly within the temperature range 750 – 850 °C. Welding with a high heat input leads to slow cooling, especially in light-gauge weldments. The weld's holding time between 750 – 850 °C then increases, and along with it the risk of sigma phase formation [1].

[1] Valahia University of Targoviste, Faculty of Material Engineering and Mechanics, 130004 Targoviste, Romania. E-mail: poinescua@yahoo.com.
[2] Valahia University of Targoviste, Institute of Multidisciplinary Research for Science and Technology, 130004 Tagoviste, Romania. E-mail: mihai.simona@yahoo.com.

An aid in determining which structural constituents can occur in a weld metal is the Schaeffler-de-Long diagram (Fig. 1). With knowledge of the properties of different phases, it is possible to judge the extent to which they affect the service life of the weldment. The diagram can be used for rough estimates of the weldability of different steel grades as well as when welding dissimilar steels to each other.

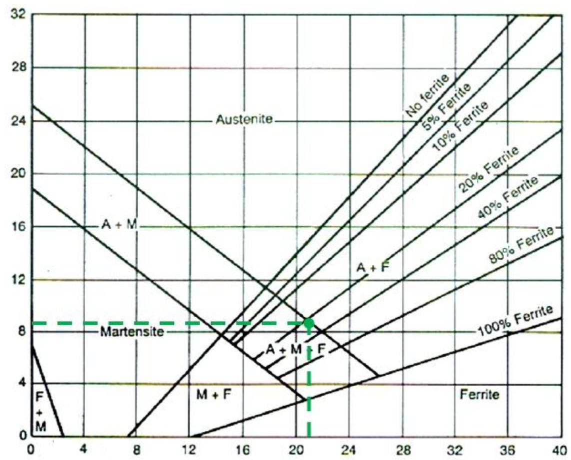

Figure 1. The Schaeffler-de-Long diagram [1].

Nanoindentation need to be accurate because there is the possibility to occur some errors in making hardness tests include:

1. Making an indentation too close to an edge of the material. If the plastic zone around an indenter extends to an edge, the reading will be too low;

2. Making an indentation too close to a prior indentation. If the plastic zone around an indenter overlaps that prior indentation, the strain hardening during the prior test will cause the new reading to be too high.

3. Making too large an indentation on a thin specimen. If the plastic zone penetrates to the bottom surface, the reading will be in error [3, 4]. The process itself consists in pressing an indenter (the top may be conical, spherical or pyramidal) of hard material (e.g. diamond) on the surface of the material, to a maximum preset force, followed by raising the tip, monitoring the force and respectively the peak movement.

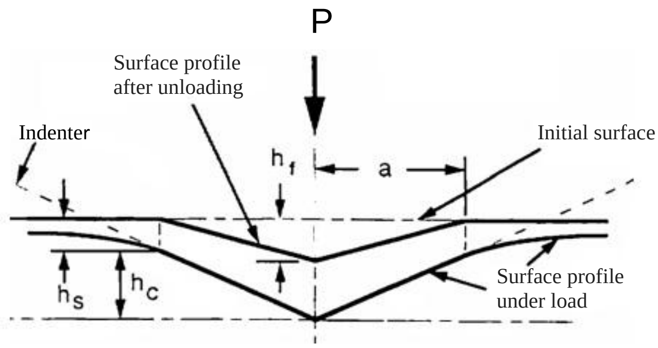

Figure 2. Indentation depth [5].

With a high-resolution test equipment like G200, estimates can be made on a micro or nanometric scale. As characteristics, the material analyzed is considered to be monolithic, associated with a semi-infinite elastoplastic space. Materials are also considered to have no time dependent deformation mechanism such as creep or viscoelasticity. To calculate the hardness and redus module was used the Oliver – Pharr method [6]. In the Fig. 2 is highlithed the depthness of indentation.

2. MATERIALS AND METHODS

2.1. MATERIALS

The material chosed for investigation was 301 stainless steel welded. Chemical composition of the material is presented in the Table 1. Welding was done by the WIG method, wolfram electrode and inert gas (high purity argon), using an austenitic-ferrite steel wire as input material [7].

After welding and cooling the sheets were cross-sectioned on the welding line and the samples thus obtained were polished and attacked with chemical reagents, to highlight the welding macrostructure [8, 9]. Stainless steel sheets 301 welded with thickness of 0.15 mm were investigated on the welding point, on the thermal influence zone and on the base material, in order to observe the changes occurring in the structure and the properties of materials due to thermal influence [10-12].

Table 1. Chemical composition of 301SS.

Chemical element	C	Mn	P	S	Si	Cr	Ni	N
Wt%	Max 0.15	Max. 2.00	Max. 0.045	Max. 0.030	Max. 0.75	16-18	6-8	0.10

2.2. METHODS

For structural analysis was used the SU-70 Electronic Scanning Microscope (SEM) coupled with energy dispesive (EDS) and wavelenght dispersive (WDS) spectrometers. The magnification range of the SEM is 30X-800,000X, and the resolution at the 15 kV acceleration voltage is 1 nm. EDS spectrometer attached allows qualitative and quantitative analysis (from Be (Z = 4) to Pu (Z = 94)) on the point, rectangle, circle or the free choice and multiple choice line analysis, X-ray mapping. WDS spectrometer attached, allows qualitative and quantitative analysis (from B (Z = 5) to Pu (Z = 94)) [13-16].

Atomic Force Microscopy technique allow surface investigations with higher resolution than usual methods and comparring with classical microscopy which give information only about two dimensional form of samples, the AFM offers a third plan of investigation [17]. Thus, it can be obtain a more accurate result regarding the shift surface in scanned area. The AFM model for this study was Ntegra Prima by NTMDT [18, 19] and, as for scanning procedure, it was used a silicon cantilever made by crystal silicon and doped with Antimony.

To analyze the hardness of the material was used Nanoindenter G200 at maximum load 500 mN [20, 21]. Calibration was carried out using fused silica as the standard calibration according ISO 14577-2 [20]. The indenter shall approach the surface at a rate of 25 nm/sec. The software used to collect and analyze data is NanoSuite.

Was performed 2 x 2 array of indentations, spaced 50 μm apart with Bercovich diamante indenter using the continuous stiffness mode with a penetrations depth of 2000 nm. For the nanointentation measurement was needed some preparation of the welded sample. The sample holder was place it on a hot plate, this become warm. After that, on the surface was spread a small amount of resin (crystalbond 509), then the metalic sample was placed to the holder and we press down. We move the slide around with wooden contact to eliminate the bubbles between the slide and sample disk. Then the metallic sample have been placed on the microscope slide.

3. RESULTS AND DISCUSSION

3.1. AFM ANALYSIS

The atomic force microscope investigations on the welded metallic sample were made in order to see the roughness of the surface before performing the nanoindentation tests [17]. Sample was investigated by Atomic Force Microscopy in Semicontact mode. Two size areas were chosen for topography analysis – 10 x 10 µm and 30 x 30 µm. In both cases, the sample shown evident marks of roughness so, additional information have been attached for this consideration as results for the obtained images (Figs. 3 and 4).

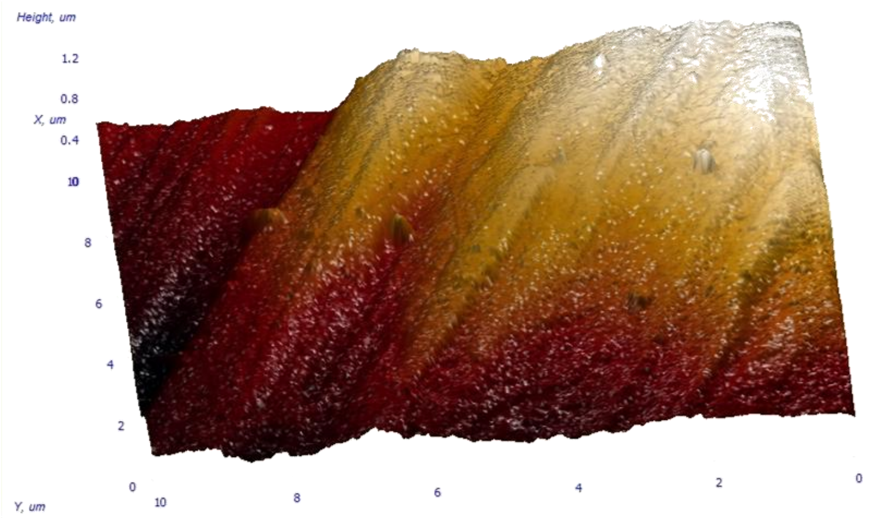

Figure 3. 301 SS - AFM investigation on base material (BM) [10x10 µm].

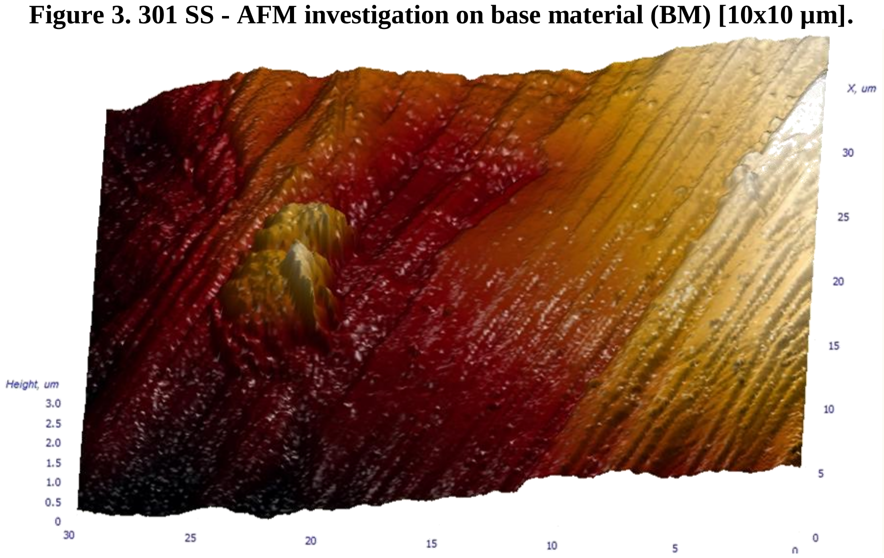

Figure 4. 301 SS - AFM investigation on Heat Affected Zone (HAZ) [30x30 µm].

AFM investigation was performed both on heat affected zone and base material, and obtained values are shown in Table 2.

Table 2. Value of roughness on investigation zone

Investigation Zone	Average roughness
HAZ	0.216 [μm]
MB	0.250 [μm]

3.2. SEM-EDS ANALYSIS

The sample was studied on three areas of interest as: welding zone, thermal influence zone and base material. The obtained images are presented comparatively in the Figs. 5-7.

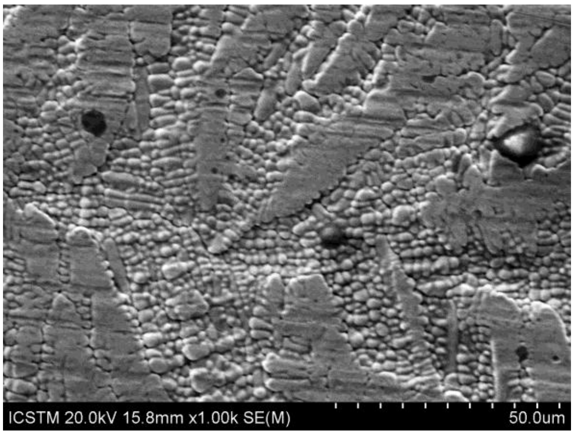

Figure 5. Welding zone (1000X) – dendritic structure.

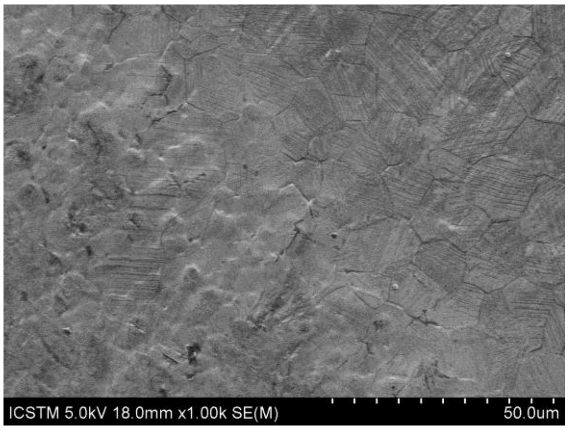

Figure 6. Thermal influence zone (1000X) – structure: ferrite and austenite.

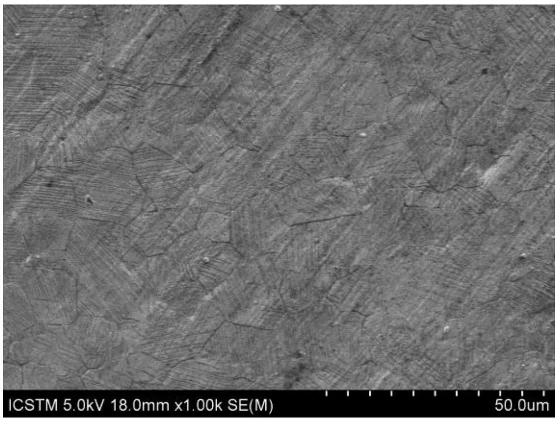

Figure 7. Base material zone (1000X) – structure: ferrite and austenite.

In the SEM images taken over the welding at 1000X magnification, it can be seen a dendritic structure obtained from the high cooling velocity for welding zone. The structure of base material is formed from ferrite and austenite.

Also, the C, Fe, Ni, Mn and Cr elements of the surface material were identified by EDS analysis and these are presented in the Figs. 8 and 9. Thus, the correlation of the elements present in the weld metal with those of the base material was established.

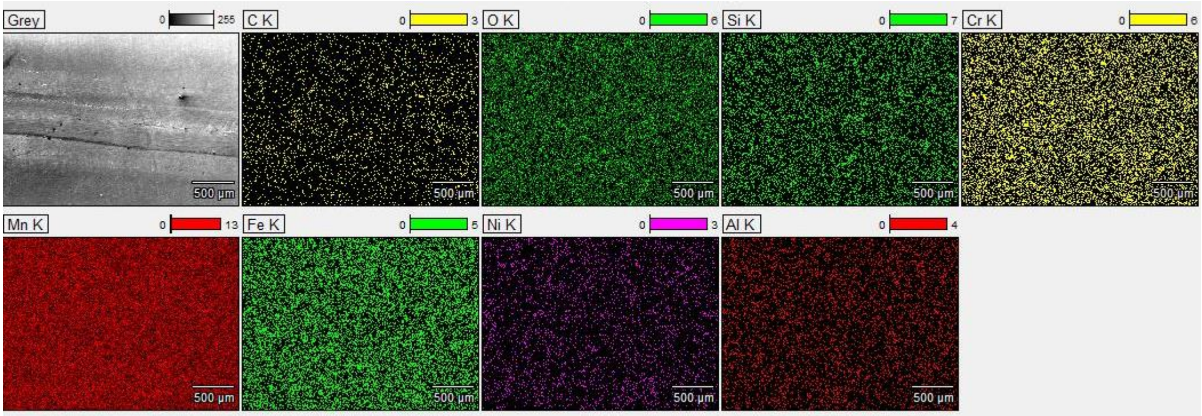

Figure 8. Distribution maps of elements on scanned area.

Elements are uniform distributed on the investigated area, and there are no differences in chemical composition between the base material and the welding zone (Fig. 8 and Table 3).

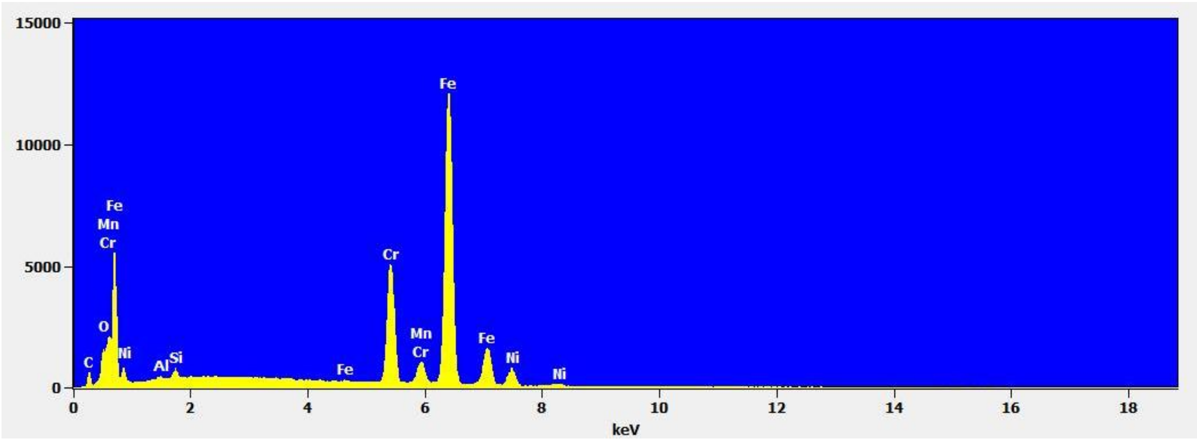

Figure 9. EDS Spectrum of investigated area.

Table 3. Elementary concentration of the studied sample

Elements	Elemental concentration on investigated area [wt.% ± wt. error]
C	4.14 ± 0.08
O	2.02 ± 0.15
Al	0.24 ± 0.02
Si	0.74 ± 0.04
Cr	16.66 ± 0.11
Mn	2.08 ± 0.07
Fe	68.33 ± 0.28
Ni	5.81 ± 0.19

3.3. NANOINTENTATION TESTS

The micro hardness evaluation was also investigated along the transverse cross section of the welding. Were determined hardness on the 6 zones as shown in the Fig. 10a. For each area 4 indentations was made, the hardness values is presented in the Table 4. Nanoindentations were made at 2000 nm depth penetration. In the Fig. 10b is presented the microscopic image of the welding plates (weld metal, heat affected zone and base material).

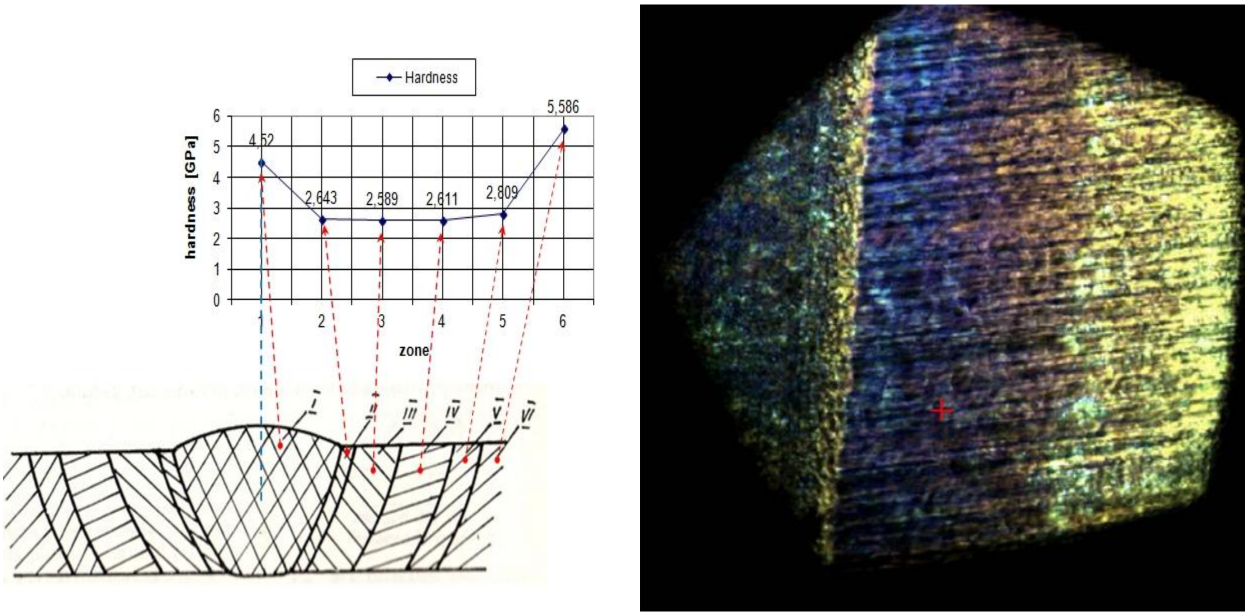

a b

Figure 10. a) Microhardness value on indented area; b) 10X Magnification image of 301 SS.

Table 4. Microhardness in different zone of welding at 2000nm depth

No.	Zone	Depth [2000 nm]	Microhardness [GPa]
1	Base material	Zone VI	5.586
2	Weld zone	Zone I	4.52
3	Heat affected zone (HAZ)	Zone II grey (between weld zone and blue zone)	2.643
		Zone III blue	2.589
		Zona IV brown	2.611
		Zona V yellow	2.809

After making all indentations, values obtained are relatively close values to the base material and the welding zone, also the values in the thermal influence zone are smaller. Fig. 11 presents the load-displacement curve on thermal influence zone. For all indentations, the nanoindenter software generate a feedback curve.

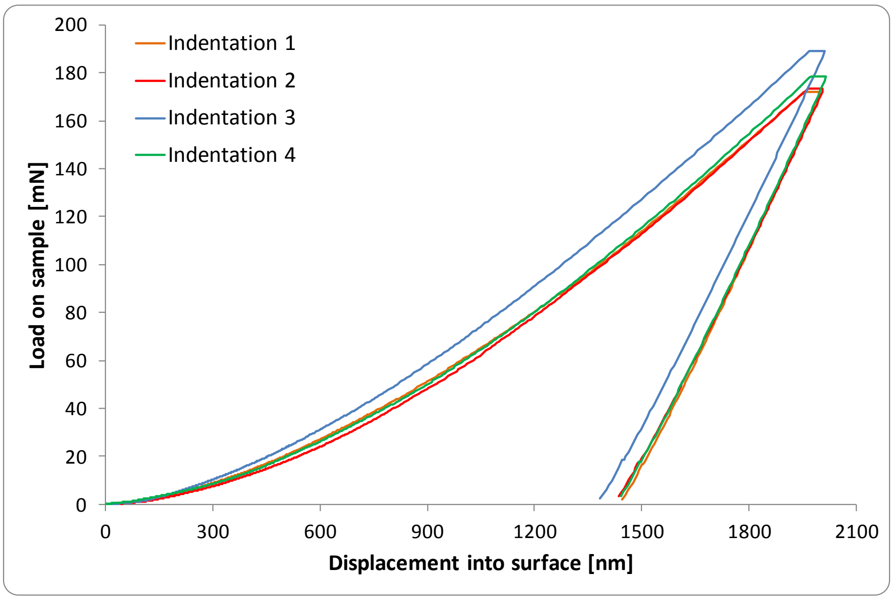

Figure 11. Load-displacement curve on thermal influence zone -yelow zone (2000nm).

4. CONCLUSIONS

If the base metal is in annealed state, practically there is no variation in structure in this area. However, if the base metal is ecruised, the neighboring section of the weld will undergo a recrystallization and grain growth. The final structure of a welded joint depends not only on the thermal cycles but also on the composition of the steel. Thus, austenitic stainless steels that do not suffer any allotropic tranformation at cooling will not show a grain reduction. Austenitic stainless steels are sensitive to overheating and become brittle in certain temperature ranges.

Austenitic steels may be sensitive to cracks due to temperature. These cracks typically occur due to eutectic alloys that are melted at low temperatures. The effect occurs when the primary austenite of the molten zone solidifies in the stainless steel. Depending on the Cr and Ni content, in austenitic steel will solidify primary ferrite and austenite. If the primary ferrite solidifies the first time, then an almost complete austenite structure will emerge by segregation and transformation. These factors have a great influence on welding and can induce material thermal cracks. If the stainless steel solidifies the primary ferrite, then the probability of thermal cracks will be very low, and if the welding parameters are appropriate.

REFERENCES

[1] Holmberg, B, *Stainless Steels - Their properties and their suitability for welding*, AvestaPolarit Welding, 2002.
[2] Atlas Steels, *Stainless Steel Grade Datasheets*, 2013. Available online at: http://www.worldstainless.org/ .
[3] Hosford, W.F., *Mechanical Behavior of Materials*, Cambridge University Press, 2005.
[4] Yovanovich, M.M., *Micro and Macro Hardness Measurements, Correlations and Contact Models*, 44th AIAA Aerospace Sciences Meeting and Exhibit, 2006.
[5] Oliver, W.C., Pharr, G.M., *Journal of Materials Research*, **7**(6), 1564, 1992.
[6] Oliver, W.C., Pharr, G.M., *Journal of Materials Research*, **19**(1), 3, 2004.
[7] Prasad, K.S. et al., *Journal for Manufacturing Science and Production*, **14**(1), 1, 2014.
[8] American Iron and Steel Institute (Nickel Development Institute), *Welding of stainless steels and other joining methods*, 1988.
[9] Sabooni, S., Karimzadeh, F., Enayati, M.H., Ngan, A.H.W., Jabbari, H., *Materials Characterization*, **109**, 138, 2015.
[10] Prabaharan, P. et al., *Journal of Materials Research*, **29**(24), 3011, 2014.
[11] ***** ASTM International, *Austenitic Stainless Steels, Stainless Steels for Design Engineers*, 2008. Available online at: www.asminternational.org.
[12] Junqueira, R.M.R. et al., *Surface and Coatings Technology*, **201**(6), 2431, 2006.
[13] Radulescu, C. et al., *Journal of Science and Arts*, **1**(34), 77, 2016.
[14] Negrea, A. et al., *Romanian Journal of Physics*, **61**(3-4), 527, 2016.
[15] Radulescu, C. et al., *Revista de Chimie*, **68**(4), 805, 2017.
[16] Bintintan, A. , et al., *Revista de Chimie*, **68**(4), 847, 2017.
[17] Despa, V. et al., *Journal of Science and Arts*, **4**(41), 839, 2017.
[18] Suica-Bunghez, I.R. et al., *Revue Roumaine de Chimie*, **62**(6-7), 545, 2017.
[19] Bucurica, I.A. et al., *Bulletin of Materials Science* – accepted, 2018.
[20] ***** Agilent Technologies Nano Indenter G200 – User's Guide, 2015.
[21] Choi, K.J. et al., *Journal of Nuclear Materials*, **471**, 8, 2016.